

Modeling the aging kinetics of zirconia ceramics

Laurent Gremillard¹, Jérôme Chevalier*, Thierry Epicier,
Sylvain Deville, Gilbert Fantozzi

GEMPPM, UMR CNRS 5510, 20 Avenue Albert Einstein, INSA de Lyon, 69621 Villeurbanne Cedex, France

Received 25 September 2003; received in revised form 20 November 2003; accepted 28 November 2003

Available online 14 April 2004

Abstract

Yttria-stabilized tetragonal zirconia polycrystals (3Y-TZP) with different microstructures were elaborated. The isothermal tetragonal to monoclinic transformation was investigated at 134 °C in steam by X-ray diffraction, Atomic Force Microscopy (AFM) and optical interferometry. The aging kinetics were analyzed in terms of nucleation and growth, using the Mehl–Avrami–Johnson (MAJ) formalism. Numerical simulation of the aging of zirconia surfaces was also conducted to better fit the aging kinetics. The simulation shows that the exponent of the MAJ laws is controlled not only by the nucleation and growth mechanisms, but also—and mainly—by their respective kinetic parameters. Measurements of nucleation and growth rates at the surface, at the beginning of aging, and the use of numerical simulation allow the accurate prediction of aging kinetics.

© 2004 Elsevier Ltd. All rights reserved.

Keywords: ZrO₂; Aging; Modeling; Kinetics; Hip replacement prosthesis

1. Introduction

Zirconia ceramics are widely used, particularly for orthopedic applications such as femoral heads for hip prostheses. Recently the failure of a number of zirconia heads^{1,2} drawn the attention to the phenomena limiting the life-time of zirconia ceramic pieces, in particular on the aging of zirconia. Aging was first described by Kobayashi et al.³ at room temperature, zirconia is retained in a metastable tetragonal phase by the addition of stabilizing agents (e.g. yttria); the aging of zirconia consists in a return towards the more stable monoclinic phase. The transformation is martensitic in nature and occurs preferentially at the surface of tetragonal zirconia ceramics. It has been shown that the tetragonal to monoclinic (t–m) transformation at the surface of zirconia ceramics is promoted by the presence of water molecules in the environment.⁴ Being subject to a volume increase, this t–m transformation induces the formation of microcracks at the surface, and an increase of the roughness. Microcracking leads to a decrease of the mechanical properties,⁴ this could explain the failure of implants after some years in vivo. The aging should then be avoided, or at least kinetics taken into account to calculate the lifetime of zirconia pieces.^{5,6}

Numerous studies have been conducted to measure the aging kinetics of Y-TZP^{4,7–27} or Ce-TZP²⁸ (yttria or ceria-stabilized tetragonal zirconia polycrystals). Depending on the authors, the laws giving the monoclinic phase amount versus time can be either linear or sigmoidal. Until now, no real effort to rationalize these differences has been made. The most detailed studies^{18,21,22,26} have shown that the sigmoidal laws are related to nucleation and growth kinetics (nucleation of the monoclinic phase first on isolated grains on the surface, then propagation to the neighboring grains as a result of stresses and microcracks accumulation). In those cases, the kinetics can be described using Mehl–Avrami–Johnson (MAJ)²⁹ laws (Eq. (1), where the exponent n is of particular interest):

$$f = 1 - \exp - (bt)^n \quad (1)$$

where f is the monoclinic fraction and t is the aging duration. However, the exponent n given in or deduced from the literature can vary from 0.3²³ to almost 4,¹⁸ with no analysis to explain these apparent disagreements. According to Christian,³⁰ these different values of n should suggest different mechanisms. The aim of this paper is to show that this exponent n is not only characteristic of the aging mechanism (i.e. nucleation and growth), but also strongly depends on the kinetic features (mainly nucleation speed and interface—growth—speed).

* Corresponding author. Fax: +33-4-72-43-85-28.

E-mail address: jerome.chevalier@insa-lyon.fr (J. Chevalier).

¹ Material Science Division, LBNL, Berkeley, CA 94720, USA.

2. Experimental

2.1. Materials

The results concerning three batches of zirconia ceramics will be exposed. The starting powder was in each case an ultra-pure Tosoh powder, stabilized in the tetragonal phase with 3 mol% of yttria and with less than 200 ppm of impurities. The samples were processed by cold isostatic pressing at 300 MPa. For the first batch (noted Z-S₁₄₅₀), the compacts were sintered at 1450 °C for 5 h in air (heating and cooling rate: 300 °C h⁻¹), to achieve grain sizes of approximately 0.5 μm (measured by SEM according to the ASTM E112 standard) and a density of 97% of the theoretical density. For the second batch (noted Z-HIP), Hot Isostatic Pressing (HIP) was conducted after the sintering step in order to achieve full density (>99%) and the occurrence of less pores and defects. For the third batch (noted Z-S₁₆₀₀), the compacts were sintered at 1600 °C for 5 h in air (without HIP) to achieve 1 μm grain size.

2.2. Aging

The low temperature degradation was quantified by following the monoclinic content on the surface of the material versus aging time. The monoclinic content, f , was measured by X-ray diffraction (XRD) and calculated from the Garvie and Nicholson³¹ Eq. (2):

$$f = \frac{I_m\{\bar{1}11\} + I_m\{111\}}{I_m\{\bar{1}11\} + I_m\{111\} + I_t\{101\}} \quad (2)$$

where $I_j\{hkl\}$ is the area of the $\{hkl\}$ peak of the phase j measured by XRD. The X-ray penetration depth (and then the depth of the analyzed area) is around 5 μm.³²

The samples were polished with diamond pastes down to 1 μm so as to achieve a perfectly smooth surface (roughness less than 4 nm measured by the mean of an optical interferometer, Phase Shift Technology®) and to remove all surface stresses due to machining. The monoclinic phase was undetectable by XRD before aging tests.

Accelerated aging tests were conducted in steam, at 134 °C, under a pressure of 2 bar (this corresponds to a standard sterilization procedure). It has been shown that 1 h of this treatment corresponds roughly to 4 years at body temperature.³³

The optical interferometer was also used to take images of the surface of aged samples, in order to follow the surface changes during aging, particularly to investigate the appearance of monoclinic nuclei and their growth. A quantification of the number and heights of monoclinic nuclei was conducted on these images.

AFM experiments were performed on a D3100 microscope (Digital Instruments™) in contact mode, using oxide sharpened silicon nitrided probes, with an average scanning speed of 20 μm s⁻¹. AFM allowed the observation of the very first stages of monoclinic spots growth, thanks to its

improved lateral resolution as compared to optical interferometry, confirming thus the interferometry measurements.

3. Experimental results

The relationship between the amount of monoclinic phase and aging time for the three zirconia ceramics is shown in Fig. 1 (dark line correspond to the simulations performed in the present work and discussed later). The curves can be considered as nearly sigmoidal for Z-S₁₄₅₀ and Z-HIP. This

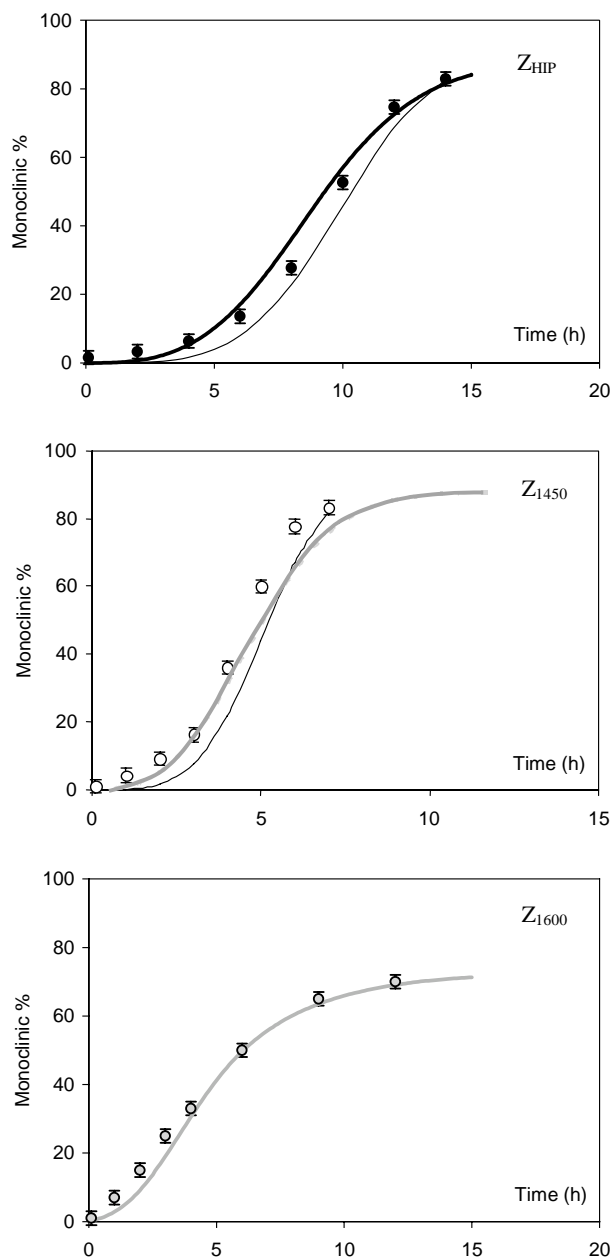


Fig. 1. Aging kinetics of zirconia ceramics. Comparison between experimental points, MAJ analytical model calculated by Chevalier et al.¹⁸ (thin lines) and simulated aging kinetics (bold lines) for the Z-HIP, Z-S₁₄₅₀ and Z-S₁₆₀₀ materials (from top to bottom, respectively).

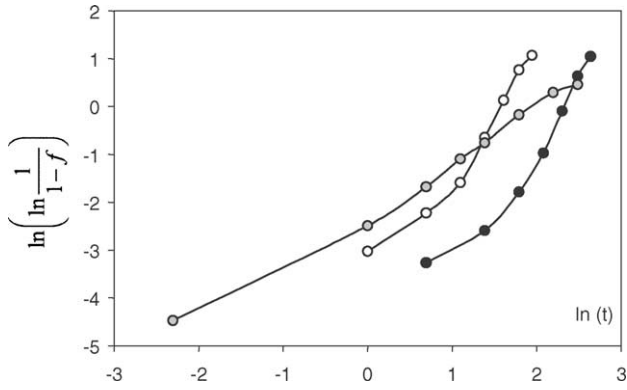


Fig. 2. Mehl–Avrami–Johnson plot of the experimental data (black: Z-HIP; white: Z-S₁₄₅₀; gray: Z-S₁₆₀₀). The slope of each curve should give the value of the exponent n in the MAJ laws.

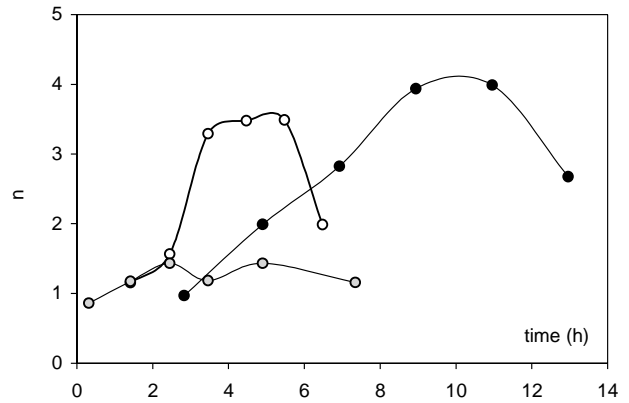


Fig. 3. Variation of the exponent n with time during the aging kinetics (black: Z-HIP; white: Z-S₁₄₅₀; gray: Z-S₁₆₀₀).

is less obvious for Z-S₁₆₀₀. The n exponent which can be derived from the slope of the $\ln(\ln(1/(1-f)))$ versus $\ln(t)$ plot of Fig. 2 varies from 1 to 4 for the three batches (see Fig. 3). According to the MAJ theory, this could suggest different mechanisms. Also the n exponent is not constant over the overall kinetic.

Recent works suggest that aging occurs in zirconia by a nucleation and growth mechanism.^{18,21} Clear evidence for this mechanism is shown by the AFM in Fig. 4. The figure shows the appearance of monoclinic nuclei, then their growth versus time in one of the tested zirconia ceramic. This was observed for the three zirconia ceramics, but with

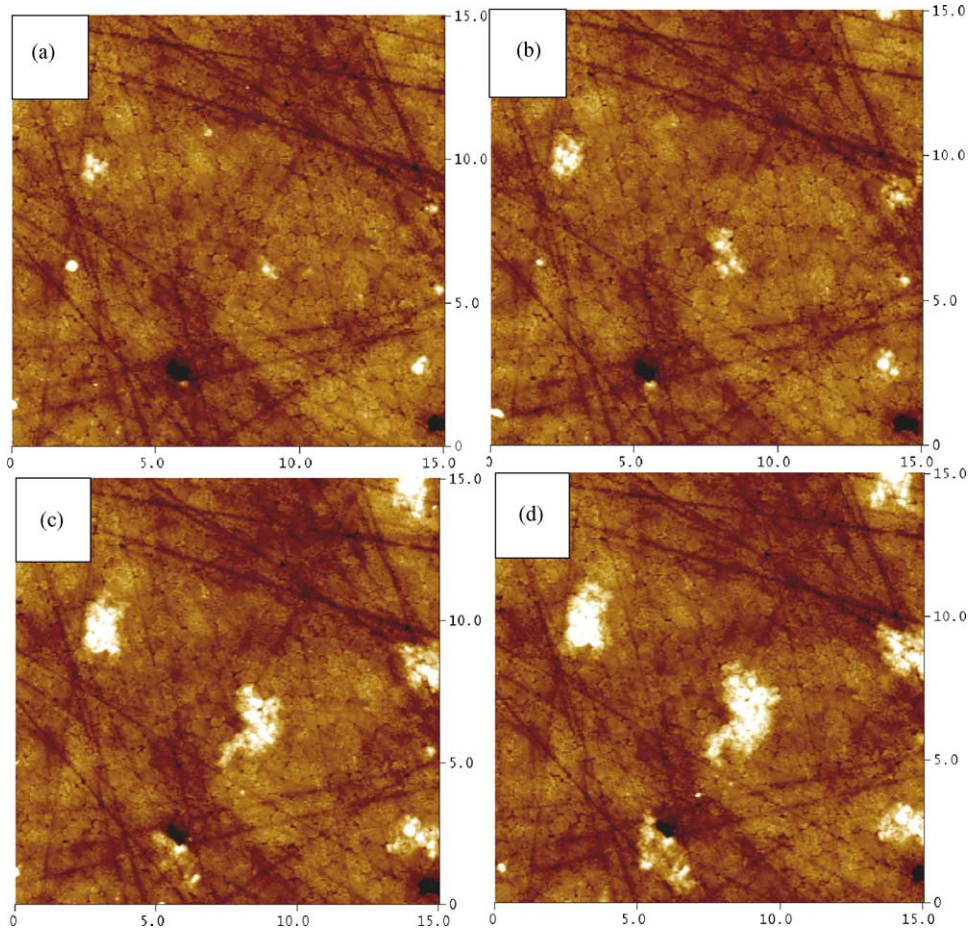


Fig. 4. AFM images ($15\ \mu\text{m} \times 15\ \mu\text{m}$) showing the initial stage of transformation at the surface of a zirconia ceramic (vertical scale contrast: 50 nm), after 30 min (a), 1 h (b), 1 h 30 min (c) and 2 h (d). Image taken in Z-S₁₄₅₀.

Table 1
Nucleation and growth parameters (N_r , α_d , α_h) and n values for the three zirconia ceramics

Batch	Z-S ₁₄₅₀	Z-HIP	Z-S ₁₆₀₀
Nucleation rate (N_r) (nuclei $h^{-1} \mu m^{-2}$)	5×10^{-3}	3.7×10^{-4}	2×10^{-2}
Diameter growth rate (α_d) ($\mu m h^{-1}$)	2.4	2.7	0.8
Height growth rate (α_h) ($nm h^{-1}$)	24	27	8
α_d/N_r	4.8×10^2	7.3×10^3	40
n (maximum recorded during aging)	3.5	4	1.4

different kinetics. In agreement with a previous study,¹⁸ we observed that the nucleation rate (number of new monoclinic regions appearing by time and by unit surface area) and the growth rate (increase of the diameter and the height of a given monoclinic region by time) were nearly constant, at least during the first hours of aging. Their values are compiled in Table 1. It is evident from these results that the nucleation rate is strongly influenced by the grain size (the higher the grain size, the higher the nucleation of new monoclinic regions) and the density (even small defects acting probably as nucleation sites). These results show that aging kinetics are strongly affected by the microstructure and confirm that decreasing the grain size and increasing the density by HIP is a good way to decrease the aging kinetics of zirconia. In particular, we show that the nucleation rate is divided by a factor of about 20 by the HIP process.

4. Models

4.1. Mehl–Avrami–Johnson (MAJ) laws for nucleation and growth

MAJ equation has often been used to fit experimental aging kinetics observed in zirconia ceramics.^{18,21–23,26} Although initially proposed for precipitation in metallic alloys, then crystallization in polymers, it could apply also to aging of zirconia, since it clearly occurs by nucleation and growth. One analytical modeling of zirconia aging kinetics was conducted in Ref. 18, leading to a MAJ type equation for the monoclinic fraction versus time. Fig. 5 shows

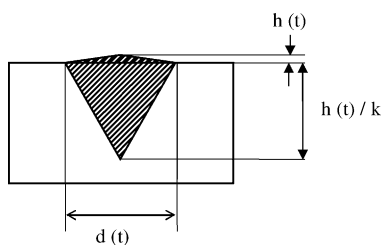


Fig. 5. Geometry of a transformed nucleus, side view (left) and extension of the transformation, top view (right).¹⁸

schematically the geometry of the transformed spots appearing on the surface in zirconia (see Ref. 18 for justification of this shape). From the current experimental results and previous works,^{18–21} it is recognized that aging occurs by a constant nucleation of new sites with time and an increase in diameter and height of existing ones at constant rate, providing their is enough space to grow. With these features, the monoclinic fraction, f , versus time, t , equation should be on the form:¹⁸

$$f = 1 - \exp \left[- \left(\frac{\pi \alpha_d^2 \alpha_h N_r}{48kl} \right) t^4 \right] \quad (3)$$

where α_d and α_h are the diameter and height growth rates, N_r is the nucleation rate, k is the linear expansion accompanying the t–m transformation (1.3%)^{18–34} and l is the X-ray penetration depth (5 μm).

This MAJ type kinetic was successfully applied to one zirconia¹⁸ and can apply well to fit the results of Z-HIP and moderately of Z-S₁₄₅₀ (see Fig. 1). However, this equation considers that the n exponent is constant, equal to 4, while experimental results show a significant variation of n with time. Moreover, this equation does not apply to Z-S₁₆₀₀, where the value of n is around 1 (no attempt was made to fit the experimental results with Eq. (3)). In the case of this latter material, the ratio of nucleation rate on growth rate is much more important (see Table 1), so that most of the monoclinic fraction created during aging is due to nucleation. The interaction between nuclei occurs rapidly, which hinders their growth. This is not taken into account in this analysis and could explain some small n values presented in the literature. Another important issue is probably the fact that the nuclei have already a size when they appear^{35,36} (they are not infinitely small as considered in the previous calculus). At last, the X-ray absorption profile is not considered. These different problems can only be solved with a numerical simulation.

4.2. Numerical simulation

In order to better model the X-ray diffraction results obtained in the three materials, a numerical simulation was conducted.³⁷ The program provides a calculation of the transformed fractions versus time, knowing the nucleation rate, the growth speed (N_r , α_h or α_d), but also the initial size of the nuclei (diameter D). Only a few simple rules must be considered:

- the nuclei are cone-shaped (Fig. 5);
- the number of new nuclei during a given time interval dt is proportional to dt , to the non-transformed surface and to the initial nucleation speed;
- the new nuclei are distributed randomly on the non-transformed surface (if the nucleus generated on an already transformed area, the software will put it on another location);

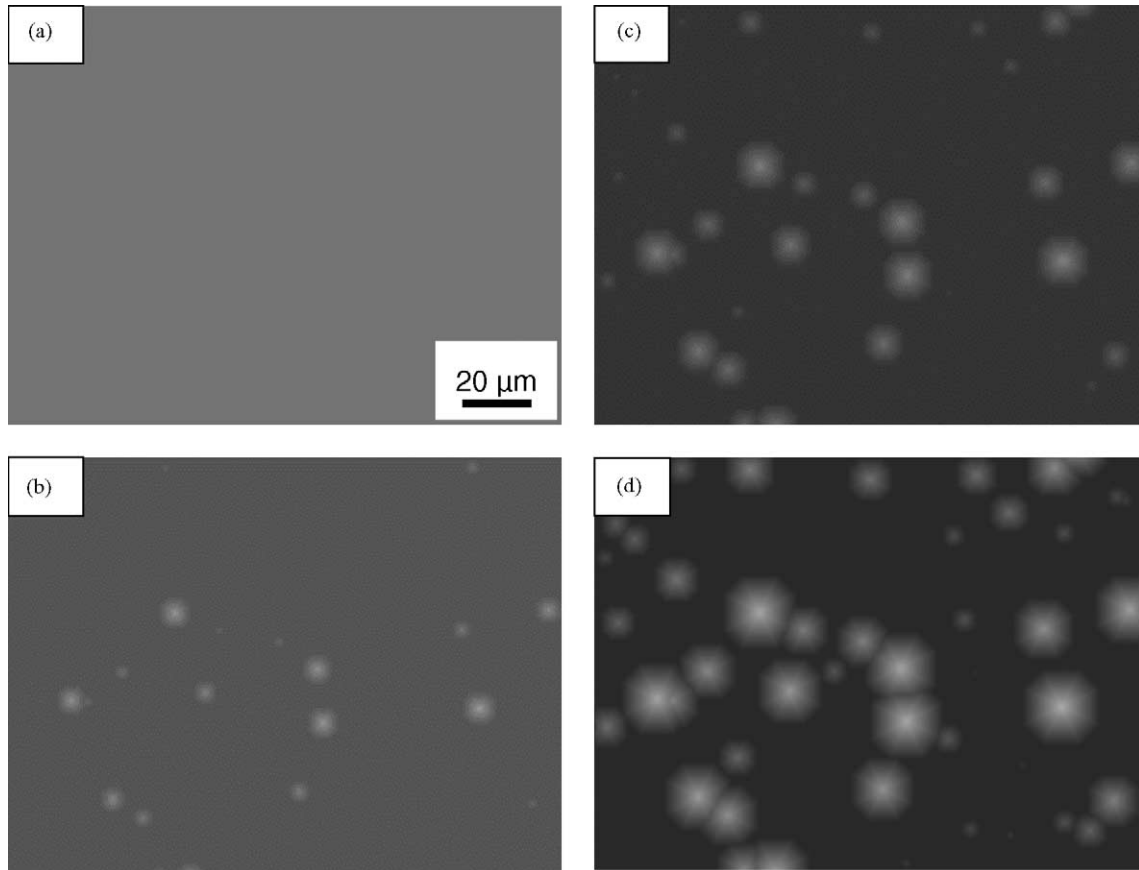


Fig. 6. Simulated images of the surface of Z-HIP after 0h (a), 3h (b), 5h (c) and 7h (d).

- the growth speed α_d is constant, and during each dt , all the points inside a given radius ($\alpha_d \times dt/2$) from the previously transformed areas are transformed;
- the transformed depth under a point of the surface is proportional to the growth speed and to the time from the first transformation;
- the X-ray absorption in the material is considered, so that the curves provided by the program can directly be compared to the aging kinetics measured by X-ray diffraction.

Each time step in the simulation is divided in a nucleation-type calculation, then a growth-type calculation. The initial state of the simulated material is completely ‘transformation free,’ and its whole surface is susceptible to transformation.

An example of images of the surface calculated by means of this simulation is given in Fig. 6.

5. Experimental validation of the numerical model

Fig. 1 provides a comparison between the experimental X-ray diffraction results and the numerical simulation conducted from the parameters of Table 1. In the simulations, D was taken as the grain size (i.e. $0.5 \mu\text{m}$ for Z-S₁₄₅₀ and Z-HIP or $1 \mu\text{m}$ for Z-S₁₆₀₀). They show in each case a

good agreement. From the simulated laws, we can derive an n exponent which could be used to fit these curves by a MAJ law: by tracing $\Delta[\ln(\ln(1/1 - f(t)))]/\Delta(\ln(t))$ versus time (Fig. 7), we obtain a curve with a plateau giving the value of the exponent n . This figure leads us to a few commentaries. First, the value of n is ranging between 1 and 4. Second, this value is not constant during aging; this is coherent with what is observed experimentally: indeed

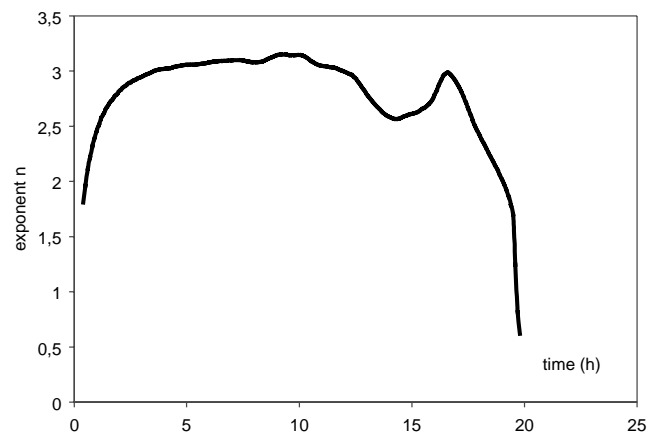


Fig. 7. Variation of the exponent n with time during a simulated aging kinetic for Z-HIP.

Fig. 3 shows the same evolution of n versus time (ascending phase, plateau and decrease) for the experimental measurements. The numerical simulation provided here is therefore much more precise than MAJ equations to model aging kinetics.

6. Discussion

In order to understand the influence of the kinetic parameters (α_h , α_d and N_r) on the shape of the sigmoidal laws (in other words on the value of the exponent n), a set of more than 200 simulations was conducted. From all the results, the exponent n is calculated according to the method previously exposed. The Fig. 8 shows that this exponent is strongly related to the proportion of newly transformed phase appearing by nucleation compared to the one appearing by growth of existing nuclei. The former quantity is proportional to the nucleation rate N_r and to the square of the monoclinic spots initial diameter (D^2). The latter quantity is proportional to the growth speed (α_d). Thus, the pre-cited proportion is proportional to $\alpha_d/N_r D^2$. Assuming that the initial diameter of the monoclinic spots is the grain size, the experimental data seems to follow the tendency given by the simulation. Fig. 8 may also allow us to explain the evolution of n during an aging kinetic (Fig. 2). We may explain the lower value of n at the beginning of aging by a stronger influence of the nucleation (equivalent to a small value of $\alpha_d/N_r D^2$). Indeed, the first nuclei are small, and their growth produces less transformed material than the growth of older nuclei. On the plateau, the proportion of transformed material appearing by nucleation and by growth is constant. The decrease and peak of the simulated n near the end of the aging curves is due to side effects (as the software does not work with an infinite material, but with an area of 2048×2048 points). This analysis is confirmed by Fig. 9. This figure plots the evolution of n during some simulations on the material Z-HIP versus the proportion of new monoclinic phase created by growth and by nucleation (dfg/dfn). This curve shows that the variation

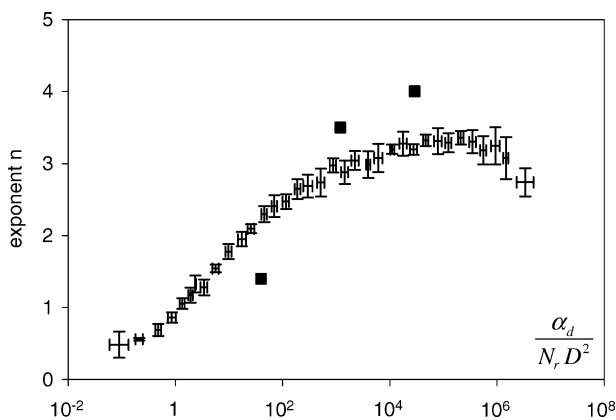


Fig. 8. Variation of the exponent n with the kinetic parameters; the black squares indicate the experimental points.

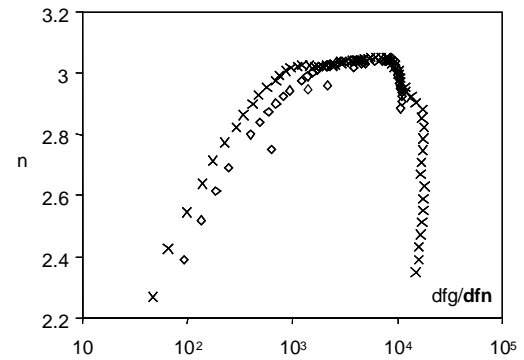


Fig. 9. Variation of the exponent n vs. the ratio of new phase appearing by growth (dfg) to the one appearing by nucleation (dfn). This is derived from two simulations for Z-HIP.

of n versus dfg/dfn inside a simulation (i.e. for a same material) is of the same kind as the one shown in Fig. 8.

From all these results, it is obvious that only numerical simulation allows to fit the aging kinetics, whatever the ratio of nucleation on growth rate. Numerical simulation can be powerful in terms of lifetime prediction, since recording the initiation of aging (nucleation and growth rate at the very beginning of transformation) by the means of AFM or optical interferometer allows the overall aging kinetics to be predicted with excellent accuracy.

7. Conclusion

This study aimed at clarifying the nucleation and growth kinetics of zirconia ceramics aging. It has been shown that in some cases MAJ laws with an exponent 4 led to a good analysis of this phenomenon.¹⁸ But in most cases, the exponents calculated from the literature data were widely inferior to 4, typically between 0.3 and 3.5. Numerical simulations allowed us to explain this fact. They showed that:

- the MAJ laws exponent is closely related to the ratio between nucleation rate and growth speed;
- this exponent is not constant during the aging (which is consistent with experimental data), and its evolution can be related once more to the proportion of transformed material appearing by nucleation and by growth.

Since a same mechanism can lead to very different values for n , it can be concluded that the knowledge of the MAJ laws exponent is in itself far from enough to characterize the nucleation and growth mechanism. The knowledge of nucleation rate and growth rate at the very beginning of the transformation can allow the transformation kinetics to be simulated correctly. This is particularly crucial for predictions of aging at body temperature.

In terms of impact of the microstructure on aging, it is confirmed here that decreasing the grain size and the porosity plays a beneficial role on nucleation rate, and thus on aging resistance. In particular HIP should be conducted on zirconia

pieces, for example prostheses, in order to increase their resistance to aging.

It is suggested that the reasoning on nucleation and growth kinetics and their influence on MAJ laws is not be limited to the study of zirconia ceramics aging. This kind of simulation can help to study any phenomenon comprising nucleation-and-growth kinetics.

References

1. <http://www.prozyr.com>.
2. <http://www.fda.gov/cdrh/recalls/zirconiahip.html>.
3. Kobayashi, K., Kuwajima, H. and Masaki, T., *Solid State Ionics* 1981, **3/4**, 489–493.
4. Sato, T., Ohtaki, S., Endo, T. and Shimada, M., In *Advances in Ceramics, Vol 24: Science and Technology of Zirconia III*. American Ceramic Society, 1988, pp. 501–508.
5. Whalen, P. J., Reidinger, F. and Antrim, R. F., *J. Am. Ceram. Soc.* 1989, **72**(2), 319–321.
6. Hirano, M., *Br. Ceram. Trans. J.* 1992, **91**, 139–147.
7. Sato, T. and Shimada, M., *J. Am. Ceram. Soc.* 1985, **68**(6), 356–359.
8. Wang, J. and Stevens, R., *Ceram. Int.* 1989, **15**, 15–21.
9. Lange, F. F., Dunlop, G. L. and Davis, B. I., *J. Am. Ceram. Soc.* 1986, **69**(3), 237–240.
10. Yoshimura, M., Noma, T., Kawabata, K. and Somiya, S., *J. Mater. Sci. L.* 1987, **6**, 465–467.
11. Lepisto, T. T. and Mäntylä, T.A., *Ceram. Eng. Sci. Proc.* 1989, **10**, 658–667.
12. Narita, N., Leng, I., Inada, S. et al., In *Sintering 87: Proceedings of the Fourth International Symposium on Science and Technology of Sintering, Tokyo, Japan*, ed. S. Somiya, M. Shimada, M. Yoshimura and R. Watanabe. Elsevier, London, 1988, pp. 1130–1135.
13. Schmauder, S. and Schubert, H., *J. Am. Ceram. Soc.* 1986, **69**(7), 534–540.
14. Li, J. F. and Watanabe, R., *J. Mater. Sci.* 1991, **32**, 1149–1153.
15. Li, J. F. and Watanabe, R., *J. Am. Ceram. Soc.* 1998, **81**(10), 2687–2691.
16. Yasuda, K., Goto, Y. and Takeda, H., *J. Am. Ceram. Soc.* 2001, **84**(5), 1037–1042.
17. Chevalier, J., Cales, B. and Drouin, J. M., *Key Eng. Mater.* 1997, **132–136**, 635–638.
18. Chevalier, J., Cales, B. and Drouin, J. M., *J. Am. Ceram. Soc.* 1999, **82**(8), 2150–2154.
19. Gremillard, L., Epicier, T., Chevalier, J. and Fantozzi, G., *Acta Mater.* 2000, **48**, 4647–4652.
20. Gremillard, L., Chevalier, J., Epicier, T. and Fantozzi, G., *J. Am. Ceram. Soc.* 2002, **85**(2), 401–407.
21. Tsubakino, H., Kuroda, Y. and Niibe, M., *J. Am. Ceram. Soc.* 1999, **82**(10), 2921–2923.
22. Tsubakino, H., Sonoda, K. and Nozato, R., *J. Mater. Sci.* 1993, **12**, 196–198.
23. Li, J., Zhang, L., Shen, Q. and Hashida, T., *Mater. Sci. Eng. A* 2001, **297**, 26–30.
24. Jue, J. F., Chen, J. and Virkar, A., *J. Am. Ceram. Soc.* 1991, **74**(8), 1811–1820.
25. Lu, H. Y. and Chen, S. Y., *J. Am. Ceram. Soc.* 1987, **70**(8), 537–541.
26. Whu, W. Z., Lei, T. C. and Zhou, Y., *J. Mater. Sci.* 1993, **28**, 6479–6483.
27. Lilley, E., In *Corrosion and Corrosive Degradation of Ceramics, Vol 10: Ceramics Transformation*, ed. R. Tressler and M. McNallan. 1990, pp. 387–406.
28. Sato, T. and Shimada, M., *Am. Ceram. Soc. Bull.* 1985, **64**(10), 1382–1384.
29. Johnson, W. A. and Mehl, R. F., *Trans. Am. Inst. Min. Metall. Pet. Eng.* 1939, **135**, 416–441.
30. Christian, J. W., *The Theory of Transformations in Metals and Alloys (2nd ed.)*. Pergamon Press, Oxford, UK, 1965, pp. 1–19.
31. Garvie, R. C. and Nicholson, P. S., *J. Am. Ceram. Soc.* 1972, **55**, 303–305.
32. Emsley, J., *The Elements (2nd ed.)*. Oxford University Press, Oxford, UK, 1991.
33. Chevalier, J., Drouin, J. M. and Cales, B., *Bioceramics* 1997, **10**, 135–138.
34. Kelly, P. M. and Ball, C. J., *J. Am. Ceram. Soc.* 1986, **65**, 242–246.
35. Deville, S. and Chevalier, J., *J. Am. Ceram. Soc.* 2003, **86**(12), 2225–2227.
36. Heuer, A. H., Chaim, R. and Lanteri, V., *Advances of Ceramics, Vol 24: Science and Technology of Zirconia III*, ed. S. Somiya, N. Yamamoto and H. Yanagida. American Ceramic Society, Westerville, OH, 1988, pp. 3–20.
37. Gremillard, L., *Microstructure-Durability Relationships in a Biomedical Grade Zirconia Ceramics*. Ph.D. Thesis, National Institute of Applied Sciences of Lyon, Lyon, France, 2002 (in French).